SUPERHEATING AND BOILING OF WATER IN HYDROCARBONS AT HIGH PRESSURES*

C. T. AVEDISIAN

Sibley School of Mechanical and Aerospace Engineering,
Cornell University, Ithaca, NY 14853, U.S.A.

and

I. GLASSMAN

Department of Mechanical and Aerospace Engineering,
Princeton University, Princeton, NJ 08544, U.S.A.

Abstract—The boiling of water drops superheated in some nonvolatile liquid *n*-alkanes was experimentally investigated at ambient pressures up to 4 MPa. It was found that boiling appeared to be initiated at the water–hydrocarbon interface by either growth of a single bubble or by streams of bubbles being released from the interface. The temperature at which boiling was first observed was found to be relatively insensitive to pressure, increasing only about 40 K over a 4 MPa change in pressure.

A qualitative theory based on the homogeneous nucleation of bubbles within superheated liquids is used to explain the effect of boiling pressure on temperature. The two observed boiling modes are justified in terms of consideration of the surface and interfacial free energies of the water and hydrocarbon, and qualitative agreement between the measured and predicted variation of nucleation pressures with temperature is demonstrated. The information obtained was used to provide insight into the mechanism by which the disruptive combustion or 'microexplosion' of burning water-in-fuel emulsified droplets would be initiated in high pressure combustion applications.

NOMENCLATURE

a,	Peng–Robinson constant, equation (11);
A,	constant defined in equation (13);
b,	Peng–Robinson constant, equation (12);
B,	constant defined in equation (14);
$E(n^*)$,	symbol for a vapor nucleus containing n^* molecules;
J,	nucleation rate;
k,	Boltzmann constant;
m_i,	molecular mass of species i;
N_{0i},	molecular number density of species i;
P,	total vapor pressure;
P_0,	liquid pressure;
P_{ie},	equilibrium vapor pressure of species i;
R,	gas constant;
T,	temperature;
T_{ci},	critical temperature of species i;
T_{cst},	water–*n*-alkane critical solution temperature;
v,	liquid molar volume;
v_{0i},	molecular volume $(v_i/6.02 \times 10^{23})$;
y,	vapor phase mole fraction;
Z,	vapor phase compressibility factor (Pv/RT).

Greek symbols

δ_{ij},	interaction parameter, equation (11);
σ,	surface tension;
σ_{12},	interfacial tension;
σ_0,	proportionality constant, equation (8);
μ,	critical exponent, equation (8);
ϕ,	fugacity coefficient.

Subscripts

i,	species i;
ie,	saturation conditions for species i;
1,	water;
2,	hydrocarbon.

1. INTRODUCTION

DIRECT contact heat transfer between a volatile and nonvolatile liquid can often result in significant superheating, followed by explosive boiling, of the volatile liquid. Important practical instances in which such explosive boiling has been observed include the spilling of liquid natural gases on water [1], the reaction between water and liquid metals [2] and the burning of water-in-oil emulsions [3]. In these situations the rapid growth of bubbles either within the volatile liquid or at the interface between the volatile and nonvolatile liquid is responsible for the explosive boiling effect.

In the absence of extraneous nucleation aids such as particles, the initial microscopic bubble whose growth leads to the observed boiling effect forms by the natural processes of homogeneous nucleation. The rate of formation of vapor bubbles which are of a size such that they are in both chemical and mechanical equilibrium with the surrounding liquid (i.e. critical

size nuclei) depends on the physical properties of the particular liquid in which the bubbles form. However, if nucleation occurs at the interface between the volatile and nonvolatile liquid, the properties of both liquids may be expected to affect the nucleation rate.

The homogeneous nucleation of bubbles within the bulk of superheated liquids has been extensively studied as has been reviewed by Blander and Katz [4]. The experimental study of bubble nucleation at a liquid–liquid interface has received much attention [5–8] and no work has been reported at pressures above atmospheric. The experimental evidence seems to indicate that, at atmospheric pressure, nucleation and growth of bubbles at a liquid–liquid interface is typically characterized by a string of bubbles emerging from the interface between test drop and field liquid [5, 7–9], instead of the characteristic explosive boiling attendant to homogeneous nucleation of bubbles within the interior of a liquid [4, 9, 10].

In the present work we report the results of an experimental program in which we attempted to measure the incipient boiling pressure at various temperatures of water drops superheated within nonvolatile hydrocarbon field liquids. The properties of the hydrocarbons were selected such that nucleation of bubbles at the water–hydrocarbon interface would be more likely to occur than within the bulk of the water drops. The information obtained was used to provide insight into the mechanism by which disruptive burning or 'microexplosion' of water-in-oil emulsified drops would be initiated during droplet combustion.

The objectives of this work were to investigate (1) the manner in which water drops boiled in some nonvolatile n-alkanes; (2) the variation of boiling temperature with pressure; and (3) the relationship between nucleation theory and the experimental observations.

2. EXPERIMENT

2.1. Description of the apparatus

Water drops were injected into a column filled with a lighter nonvolatile liquid hydrocarbon under pressure and at a uniform temperature. The initial pressure was set equal to the saturation pressure of water at the hydrocarbon temperature to insure intimate liquid–liquid contact between water and hydrocarbon at the start of an experiment. As the heavier water drops fell, they were superheated by releasing the pressure on the hydrocarbon. When a water drop which had been arbitrarily selected for observation by the naked eye began to boil, the pressure and temperature of the fuel were recorded on a chart recorder by remotely activating an event marker button. A variation of this isothermal decompression method was used by Moore [6] to measure the limit of superheat of pure freon-12 in water as a function of pressure, and by Forest and Ward [11, 12] for measuring the limit of superheat of ethyl ether–nitrogen solutions in a flowing stream of glycerine.

A schematic diagram of the experimental installation is shown in Fig. 1. The apparatus consisted of a double chamber configuration in which an inner test section containing the hydrocarbon was mounted within an outer pressure vessel. Slotted windows on the pressure vessel with direct back lighting provided visual access to the interior of the test section. The test section essentially consisted of a glass tube (45 mm O.D., 41 mm I.D. and 450 mm long) which was closed at one end. The open end was sealed by a stainless steel cap with O-rings. The tube was heated by two aluminum blocks with variac regulated electrical strip heaters attached along its length. The test section assembly was hung from the underside of the top cover plate of the pressure cell, and all wires were passed through Conax 'feedthrough' fittings screwed into the top cover plate. Filtered nitrogen gas was used to pressurize the fuel and was in contact with it only at an external reservoir. This reservoir was placed approximately 1.14 m from the pressure cell in order to minimize the amount of nitrogen gas dissolved in the liquid in the test section.

The water injection system consisted of an external reservoir connected to a stainless steel capillary tube (0.13 mm I.D. and 1.6 mm O.D.), one end of which was passed through a heat exchanger T-fitting mounted on the top cover plate and into the top of the test section, and the other end of which was connected to a solenoid valve. The water was pressurized by nitrogen gas in contact with the free liquid surface in the reservoir, and the reservoir was connected to the solenoid valve by a length of standard 6.3 mm stainless steel tubing 1.14 m long. A high pressure Millipore filter holder containing a 0.45 μm filter was attached to the outlet of the water reservoir. By pressurizing the water reservoir from 30 kPa to 70 kPa higher than the pressure in the test section, and then quickly opening and closing the solenoid valve, a group of drops typically under 3 mm in diameter could be forced through the capillary tube and into the fuel.

As the water drops fell, the pressure was released by manually opening a ball valve. When a water drop which had been selected for observation from among the group of falling drops was observed to emit bubbles or change its direction of motion, an event marker on a chart recorder was remotely activated by pushing a button, thus giving a record of the pressure and temperature of boiling. Temperature was recorded by two thermocouples located at fixed positions 70 mm and 180 mm from the top of the glass tube test section. Whenever possible, the decompression rate was regulated in a manner such that the water drops boiled between the two thermocouples whose temperatures differed by less than 0.5 K. The pressure was recorded by a transducer connected to one of two channels on the chart recorder; the other channel was connected to the lower of the two thermocouples in the test section. A new temperature was selected and the procedure repeated. In this manner it was possible to measure the variation of boiling pressure with tem-
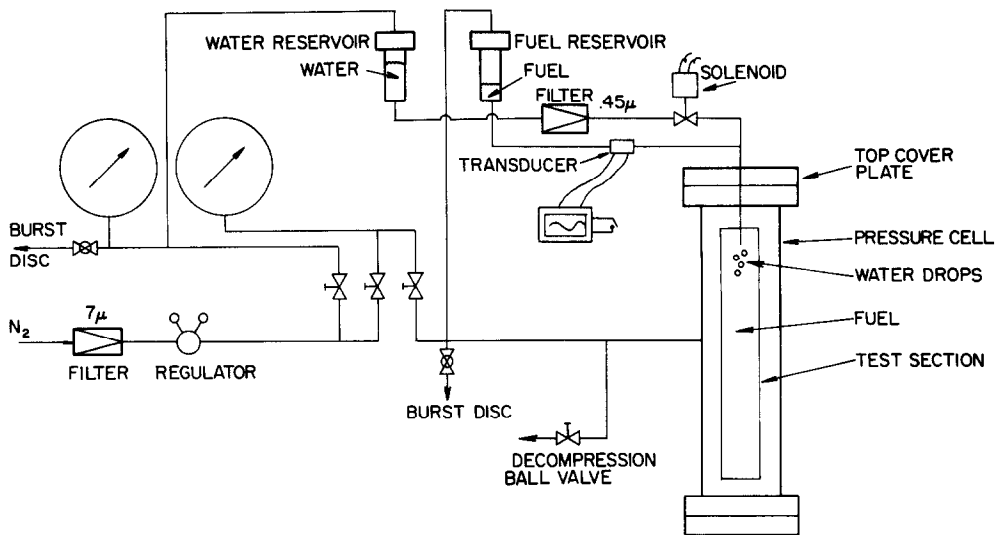
FIG. 1. Schematic diagram of the apparatus.

perature of the water drops. Further discussion of the apparatus and procedure for obtaining the data are described in more detail elsewhere [13].

2.2. Choice of liquids

Because of their relatively low surface tension, high interfacial tension with water, nonvolatility, the availability of relevant property data, and their relatively low solubility with water, the hydrocarbons selected as the field liquid were n-decane, n-pentadecane and n-hexadecane. Mixtures of these n-alkanes with Span 85 (available from Atlas Chemical Co.) were also used in order to assess the affect of a low interfacial tension on the nucleation pressure. The hydrocarbons were obtained from Humphrey Chemical Co. with a stated purity of >99% and were used directly as received without degassing or further purification except for normal filtering. The water was tap water which was distilled twice in an all-glass apparatus.

2.3. Experimental observations

The water drops were observed to boil by: (1) nucleation of a single bubble; and (2) emitting tiny bubbles from the water–n-alkane interface. Figures 2 and 3 show examples of these two boiling modes, respectively, for a water drop in pure n-hexadecane. Similar results were also observed in n-decane and n-pentadecane.

The series of photographs in Fig. 2, taken from a sequence of motion picture frames (400 frames/s), shows the growth of a single vapor bubble at the water–hydrocarbon interface. The fuel decompression rate averaged 1.4 MPa s^{-1} in this sequence so that the liquid pressure in each frame is on the average 3.4 kPa lower than the preceding frame. The water drop is

initially about 1 mm in diameter (its apparent ellipsoidal shape is due to the curvature of the glass tube). The nucleation process occurred at a time between the first and second frames. Subsequent frames illustrate the growth of the nucleated bubble. The pool of liquid which has drained around the bubble surface to form a cylindrical column in its wake, as illustrated in the nineteenth frame, shows that the water has not fully vaporized as might be expected if bubble nucleation occurred within the bulk of the water drop. The fuel temperature is well below the homogeneous nucleation temperature of the water at the ambient pressure on the hydrocarbon.

Figure 3 shows a water drop (~0.9 mm dia.) whose surface is covered with tiny vapor bubbles (~50 μm dia.). As the water drop falls, the nucleated bubbles are swept back and detach in the wake of the drop. Once the bubbles detach from the water–hydrocarbon interface, they change little in size: the fuel is nonvolatile compared to water and its contribution to the gas pressure within the bubble is negligible. If the bubbles remain at the interface it appears that they can grow to a much larger size (Fig. 2). This observation forms the basis of the model described in Section 3.2.

The two boiling modes appeared to be similar to the type of nucleation observed by Apfel [5], Blander et al. [9] and Mori and Komotori [14] for water drops isobarically heated in a silicone oil field liquid at atmospheric pressure. The bubble growth rate was much slower in the single bubble case in our experiments than that reported by Mori and Komotori [14]. This difference was most probably due to the fact that nucleation was initiated at a positive pressure in our experiments (in the range of 1.6–2.4 MPa for the sequence illustrated in Fig. 2), and that the n-alkane surfaces tension is lower than that of silicone oil. Both these factors could contribute to a reduced bubble growth rate. The fact that an interfacial type of
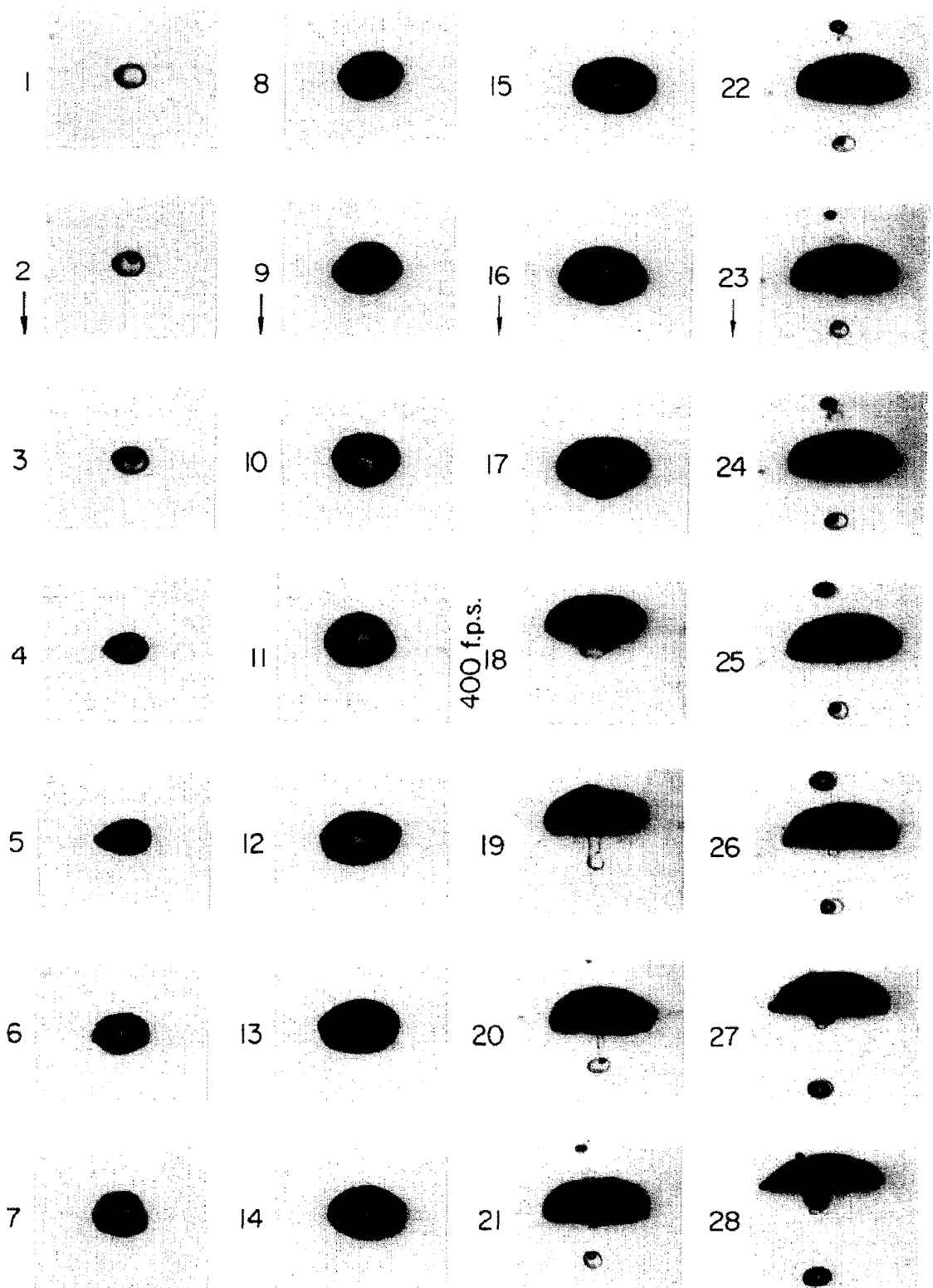
WATER DROP IN HEXADECANE , (T≈557°K)

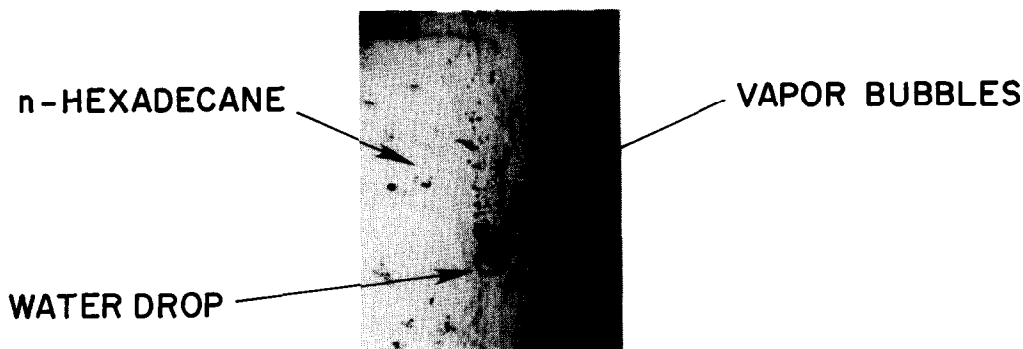Fig. 2. Photographic sequence of a water drop boiling in n-hexadecane (single bubble mode).

FIG. 3. Photograph of a water drop boiling in *n*-hexadecane (streaming bubble case).

nucleation was observed in the water–*n*-alkane systems, but not in other systems [13], may be explained by the surface forces on the initial microscopic vapor bubble as discussed later on.

The water and hydrocarbons used appeared to be nearly immiscible at room temperature. However, it became apparent, particularly in the case of water drops in *n*-decane, that some dissolving occurred at high temperatures (> 470 K). During cooling of each of the three *n*-alkanes after a series of runs, they became cloudy. This turbidity indicated that some water was dissolved in the hydrocarbon and had now separated out in the form of micron size drops. Over a period of days the cloudy mixture became clear again and water drops were visible at the bottom of the test section. This dissolving effect could help to explain why water drops would not boil in the hydrocarbon if the residence time of the drops in the fuel was large (this problem was most pronounced in *n*-decane above 509–513 K). Bubble nucleation within a solution of water and hydrocarbon would be expected to occur at a higher temperature than at the water–hydrocarbon

interface attendant to assuming immiscibility of water and hydrocarbon. This dissolving effect was minimized by adjusting the decompression rate such that the water drops remained in the fuel for under 5 s. In this way, reasonably reproducible results could be obtained.

2.4. Experimental results

The variation of the recorded boiling pressures with temperature, obtained in a series of experimental runs, is shown in Figs. 4–6 for the three *n*-alkanes we used (each data point was obtained from a single decompression).

Individual data are plotted without any averaging. There appeared to be no discernible difference in the experimental results when Span 85 was added to the *n*-pentadecane and *n*-hexadecane.

The experimentally observed pressures at which water drops boiled in *n*-decane exhibited a sufficiently wide scatter over a relatively small temperature range (Fig. 4) that no definite conclusions could be drawn about the temperature dependence of the nucleation
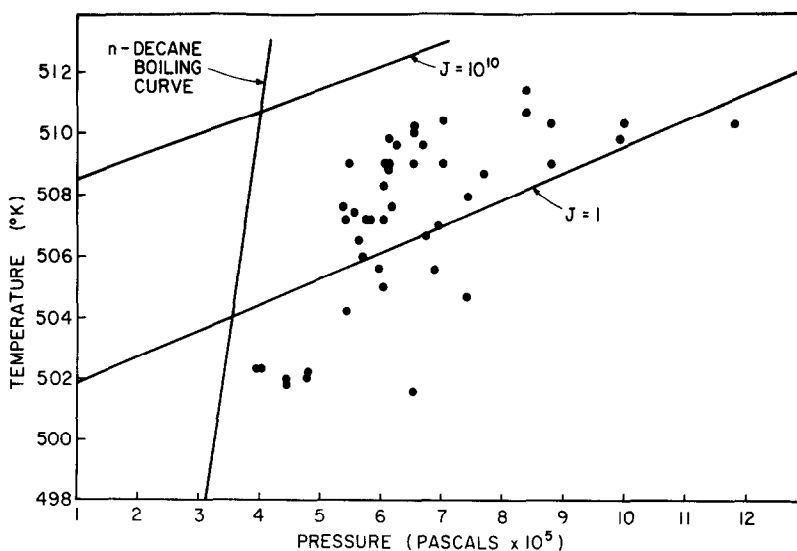

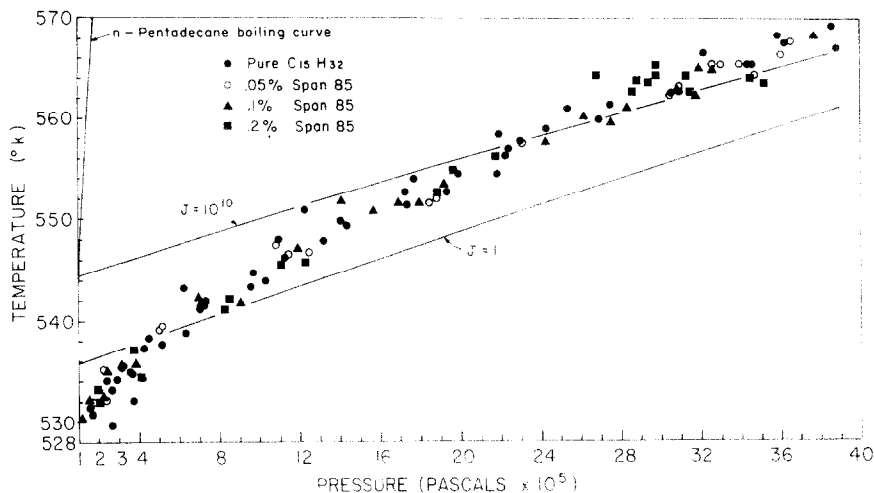FIG. 4. Nucleation temperature and pressure of water in *n*-decane.

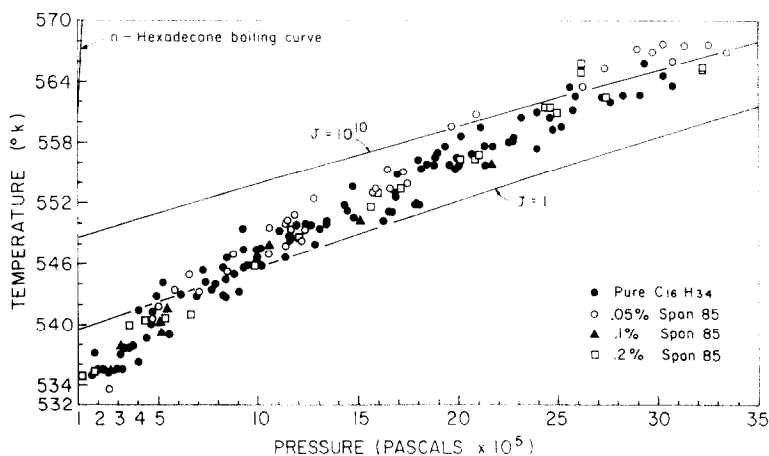FIG. 5. Nucleation temperature and pressure of water in n-pentadecane.

FIG. 6. Nucleation temperature and pressure of water in n-hexadecane.

pressure. We believe this scatter to have been due in part to the solubility problem mentioned before. The pressures at which water drops boiled in n-pentadecane and n-hexadecane exhibited a much more definite trend as shown in Figs. 5 and 6, and this effect may have been due to the lower solubility of water in these two liquids.

The nucleation temperature was found to be relatively insensitive to pressure, and increased only about 40 K over a 4 MPa change in pressure as illustrated in Figs. 5 and 6. In addition, the scatter of nucleation pressure for a given temperature was great, being typically 0.5–0.8 MPa. By contrast the pure hydrocarbon saturation temperature is much more strongly dependent on pressure. This relative insensitivity of nucleation temperature with pressure is consistent with the proposed mechanism of bubble nucleation presented in Section 3.

3. DISCUSSION

### 3.1. Nucleation temperature

In the absence of a pre-existing gas phase, a liquid-vapor phase transition within the bulk of a liquid or at a liquid–liquid or liquid–solid interface will be initiated by the formation of 'seeds' or 'nuclei' of the vapor phase in bulk liquid. The growth of these vapor bubbles to an observable size defines the boiling of a liquid. Kinetic theory [15, 16] provides a means for predicting the birth rate of the initial vapor bubble. The rate of formation per unit volume or area (depending on whether or not nucleation occurs within the bulk of a liquid or at a surface) of critical size nuclei can be shown to be proportional to the exponential of the energy required to form the critical size vapor bubble. The mean temperature in the range in which the nucleation rate changes from a negligible value to a very large value is defined as the nucleation

temperature, which can be written as [13]

$$T \simeq \frac{16\pi\sigma^3}{3(P - P_0)^2} \left\{ k \ln \left(\frac{N_0 \Gamma k_f}{J} \right) \right\}^{-1} \quad (1)$$

where N_0 is the number density of molecules when bubble nucleation occurs within the bulk of a liquid, or the number of molecules per unit area when nucleation occurs at a liquid–liquid interface. In this latter case, we approximated N_0 as $N_{01} v_{01}^{1/3} + N_{02} v_{02}^{1/3}$. The pre-exponential factor, Γ, takes into account the detailed molecular processes by which critical size nuclei form. Experimental verification of various theoretical expressions for Γ is not possible because of the inability to observe the microscopic structure of the liquid during the nucleation process. But this fact does not pose a limitation of the usefulness of equation (1). A suitable estimate of J commensurate with experimental conditions must still be obtained (e.g. [4]) and the resulting errors could easily offset a precise determination of Γ. The fact that the main uncertainty in equation (1) lies in the logarithmic term is fortunate, and this fact will tend to minimize the effect of errors in either J or Γ as large as a few orders of magnitude in the solution of equation (1). Specific expressions for Γ can be derived within the framework of nucleation theory [13]. In practice, however, the various expressions for Γ tend to differ by under two orders of magnitude and thus insignificantly affect the nucleation temperature.

In the spirit of the absolute theory of reaction rates wherein the critical size nucleus is the activated complex, the rate of formation of bubbles is governed by the rate of the following reaction

$$E(n^* - 1) + E(1) \rightleftharpoons E(n^*) \xrightarrow{k_f} E(n^* + 1) \quad (2)$$
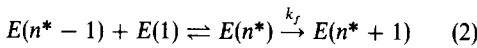
where $E(n^*)$ denotes a vapor nucleus containing n^* molecules (the critical size nucleus) and $E(1)$ denotes a single molecule. The rate constant, k_f, was approximated by the sum of the ideal gas rates of evaporation of each species within the nucleus. In the binary water–hydrocarbon systems of present interest,

$$k_f \simeq \frac{P}{\sqrt{2\pi kT}} \left(\frac{S_1 y_1}{\sqrt{m_1}} + \frac{S_2 y_2}{\sqrt{m_2}} \right) \quad (3)$$

where S_1 is the surface area of that part of the vapor nucleus on which evaporation of species 1 occurs, and similarly for S_2 (for a spherical nucleus within the bulk of a liquid $S_1 = S_2 = 4\pi r^2$ where r is the nucleus radius).

By assuming an equilibrium distribution of vapor nuclei within a superheated liquid, equation (1) can be obtained as a consequence of applying the law of mass action to equation (2), from which it is found that $\Gamma = 1$: all nuclei larger than the critical size grow and none decay.

Equation (1) can be solved once the following are known: (1) whether or not the nucleus will form within the bulk of the water or hydrocarbon or at the water–

hydrocarbon interface; (2) the surface tension, σ, of the vapor nucleus as a function of temperature; (3) the vapor pressure, P, within the nucleus; and (4) the nucleation rate.

3.2. Nucleation at the water–hydrocarbon interface

We envisage that nuclei may form at any of the five locations modelled in Fig. 7. In positions 1, 2, 4 and 5 the nucleus is spherical, while in position 3 it has a lenticular shape. In positions 2, 3 and 4 we assume that the vapor pressure within the nucleus is the sum of the partial pressures of water and hydrocarbon, and that in positions 1 and 5 the properties of water and fuel alone, respectively, characterize the energy of the critical size nucleus. The surface tensions of spherical nuclei in positions 2 and 4 are assumed to be insensitive to vapor composition and are given by the pure water and fuel values respectively. The effective surface tension of the lenticular nucleus (position 3) is [5, 7, 13]

$$\sigma_{\text{eff}} = \left[\frac{\sigma_1^3 + \sigma_2^3}{2} + \frac{\sigma_{12}^3}{16} + \frac{3\sigma_1^2 \sigma_2^2}{8\sigma_{12}} \right.$$
$$\left. - \frac{3\sigma_{12}(\sigma_1^2 + \sigma_2^2)}{8} - \frac{3(\sigma_1^4 + \sigma_2^4)}{16\sigma_{12}} \right]^{1/3} \quad (4)$$

where σ_{12} is the water–hydrocarbon interfacial tension.

The basis for expecting nucleation to occur at the water drop–hydrocarbon interface is determined by both the interfacial forces acting on the vapor lens and by assuming that the critical size bubble will form at the location where its energy is lowest [5, 7, 13]. If a lenticular nucleus is to be stable, then we must assure that

$$\sigma_{12} > |\sigma_1 - \sigma_2|. \quad (5)$$

Otherwise, if

$$\sigma_1 \geq \sigma_2 + \sigma_{12} \quad (6)$$

or

$$\sigma_2 \geq \sigma_1 + \sigma_{12} \quad (7)$$

then the nucleus is spherical (positions 2 and 4) and forms in the liquid with the lower surface tension, which in our present application is the n-alkane
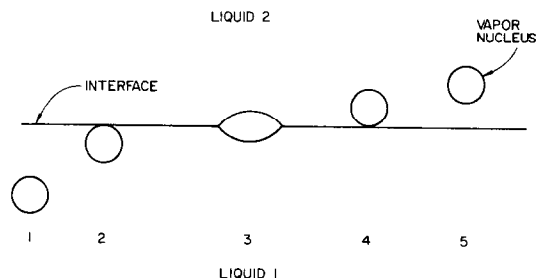

FIG. 7. Locations of nucleus formation relative to a liquid–liquid interface.

(position 4). S_1 (equation (3)) is, in this case, an arbitrarily small surface area which we have taken to be on the order of an effective cross-sectional area of a water molecule.

The n-alkane surface tensions were determined from the equation

$$\sigma_2 = \sigma_0 \left(1 - \frac{T}{T_{c2}} \right)^{\mu}. \qquad (8)$$

Values of σ_0 and the critical exponent μ, listed in Table 1, were obtained from correlations available in the literature [10, 17]. The surface tension of water was estimated from an equation given by Schmidt [18].

Equation (8) was also used for calculating the effect of temperature on the water–n-alkane interfacial tension. T_{c2} was replaced by the water–n-alkane critical solution temperature, T_{cst}, and σ_0 and μ were determined from the available interfacial tension data. Such data are scarce at high temperature. Accordingly, σ_0 and μ were estimated by averaging the available low temperature data [19, 20] over the temperature range in which measurements were reported. Table 1 lists the results, as well as the critical solution temperatures obtained by interpolating between the values reported by Connolly [21] and Sultanov et al. [22]. (It may be noticed that the physically unobtainable result $\sigma_{12} > \sigma_1 + \sigma_2$ is satisfied using the correlations listed in Table 1 for water–n-pentadecane and water–n-hexadecane above 570–580 K. We believe that this result is due to either inaccurate values of T_{cst} or to the possibility that the effect of mutual solubility of water and hydrocarbon on σ_1 and σ_2 may have to be accounted for to properly determine surface tension.)

In the absence of any surfactant which would tend to lower the interfacial tension, equation (5) is satisfied because of the relatively high water–hydrocarbon interfacial tension. Over the temperature range for which equation (5) is satisfied, $\sigma_{eff} \simeq \sigma_2$ to within 30% up to around 500 K. (At higher temperatures, the accuracy of the interfacial tension correlations may be questionable as discussed above.) As a result, we decided to use the n-alkane surface tension to charac-

Table 1

Pure hydrocarbon surface tension

Hydrocarbon	σ_0	μ	T_c(K)
n-decane	59.37	1.38	617.6
n-pentadecane	54.0	1.3	707.0
n-hexadecane	55.2	1.33	717.0

Water–n-alkane interfacial tension

Hydrocarbon	σ_0	μ	T_{cst}(K)
n-decane	81.75	0.7714	629.4*
n-pentadecane	75.38	0.5519	634.6*
n-hexadecane	75.7	0.5537	635.7†

* Carbon number average of values of T_{cst} reported in [21] and [22].
† Sultanov et al. [22].

terize the surface free energy of the vapor nucleus which, therefore, obviates the need for any water–hydrocarbon interfacial tension values in order to solve equation (1).

If the shape of the lenticular nucleus remains unchanged during its growth to observable size, then the second frame in Fig. 2 would, we believe, show that a lenticular bubble has formed at the water–hydrocarbon interface, but this is just conjecture. On the other hand, the lowering of σ_{12} attendant to the presence of Span 85 in the hydrocarbon implies that any bubble tending to form at the interface will be pushed into the hydrocarbon (position 4 in Fig. 7). Such bubbles will detach from the interface when their buoyancy force overcomes the surface tension force which holds them to the interface. This argument could be used to explain the relatively small size of bubbles streaming off the water drop shown in Fig. 3. After detachment from the interface, the bubble size is essentially frozen because the hydrocarbon is isothermal and nonvolatile. The fact that we did not notice a difference between the nucleation pressure or boiling modes of the water drops with or without surfactant in the hydrocarbon may indicate that $\sigma_{eff} \simeq \sigma_2$ over the whole temperature range in which the experiments were performed. In this case, the energy of the critical size nucleus would be the same in position 3 as in position 4, and a vapor bubble would be equally likely to form in either of these two positions. We believe this conclusion is qualitatively confirmed by our observations.

In this model of the water–hydrocarbon interface, we have neglected the thickness of the diffuse interfacial region between water and hydrocarbon compared to the diameter of the critical size nucleus. A more realistic model may be to assume that there is actually an interfacial region within which water and hydrocarbon are mutually saturated, and that the thickness of this region is much greater than a critical size nucleus. The lowest temperature at which bubble nucleation is likely to occur would then be the homogeneous nucleation temperature of water, since the hydrocarbon is relatively nonvolatile. Such superheats were not reached in our experiments. The experimental results revealed that, near atmospheric pressure, the water drops boiled at temperatures under around 540 K as shown in Figs. 4–6. This temperature is below the highest value reported in the literature of 552.7 K [23] for a liquid–vapor phase transition of water at atmospheric pressure, and well below the theoretical homogeneous nucleation temperature for water of about 575 K. Our model is only a first step toward a more complete understanding of boiling at liquid–liquid interfaces.

3.3. Vapor pressure

The partial pressure of species i within a vapor nucleus whose components are immiscible as incompressible liquids may be estimated from the following relation:

$$Py_i\phi_i = P_{ie}\phi_{ie}\exp\left[\frac{v_{ie}}{RT}(P_0 - P_{ie})\right]. \qquad (9)$$

The fugacity coefficients, ϕ_i and ϕ_{ie}, were calculated by using the Peng–Robinson [24] equation of state to express the nonideal behavior of each species within the nucleus

$$\phi_i = \exp\left(\frac{b_i}{b}(Z-1) - \ln(Z-B) - \frac{A}{2\sqrt{2}B}\right.$$

$$\left.\times\left(\frac{\sum_{j=1}^{2} a_{ij}y_j}{a} - \frac{b_i}{b}\right)\ln\frac{Z+2.414B}{Z-0.414B}\right) \quad (10)$$

where

$$a = a_1 y_1^2 + 2y_1 y_2\sqrt{(a_1 a_2)}(1-\delta_{12}) + a_2 y_2^2 \quad (11)$$

$$b = y_1 b_1 + y_2 b_2 \qquad (12)$$

$$A = \frac{aP}{R^2 T^2} \qquad (13)$$

and

$$B = \frac{bP}{RT}, \quad (i = 1, 2). \qquad (14)$$

The parameters a_i and b_i are obtained from the pure component data, and δ_{ij} is an interaction parameter for the i–j pair. In the absence of any experimental vapor pressure data for an immiscible water–hydrocarbon mixture at high temperatures and pressures, we used $\delta_{ij} \simeq 0.48$ as found by Peng and Robinson [26] for a number of water–n-alkane solutions. Values of ϕ_{1e}, calculated from equation (10), were within less than 1% of values estimated from a generalized correlation developed by Lykman *et al.* [26].

Equation (9) was solved numerically over the ranges $470\,\text{K} \leq T \leq 570\,\text{K}$ and $101\,\text{kPa} \leq P_0 \leq 4154\,\text{kPa}$ $(P > P_0)$. Values of P_{ie} for the n-alkanes and water were obtained from correlations developed by Gómez-Nieto and Thodos [27] and Keenan *et al.* [28] respectively. Saturated liquid molar volumes were estimated from a method developed by Hankinson and Thomson [29]. The results are shown in Figs. 8 and 9. Figure 9 also includes the pressure obtained by assuming the ideal gas approximation $\phi_i = \phi_{ie} = 1$ at $P_0 = 101\,\text{kPa}$. (The ideal gas pressure for the water–n-hexadecane system was nearly identical with the two curves in Fig. 8.) Although it was found that ϕ_{2e}/ϕ_2 was as high as 1.6 in the water–n-hexadecane system, the equilibrium vapor pressure of n-hexadecane is low compared to the partial pressure of water. More importantly, it was found that $\phi_{1e}/\phi_1 \simeq 1$ so that the ideal gas approximation is rather good for the vapor pressure of the water–n-hexadecane system. The increased volatility of n-decane relative to n-hexadecane resulted in a larger contribution to the total gas pressure due to the n-decane partial pressure. However, the ideal gas assumption is still not unreasonable for this system and the computation is much
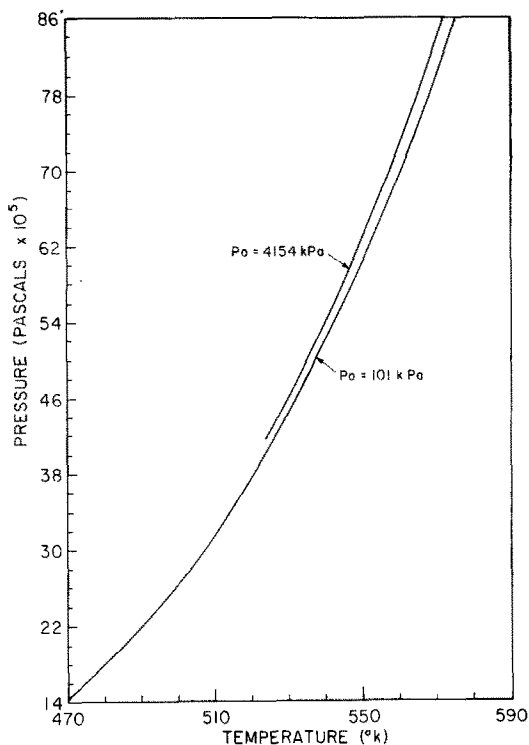

FIG. 8. Vapor pressure within a bubble at the water–n-hexadecane interface assuming immiscibility.

easier to perform; equation (9) then gives an explicit method for calculating the partial pressure of water and hydrocarbon and an iterative solution is not required.

3.4. Results

Equation (1) was solved numerically and the results are shown in Figs. 4–6. The theoretical curves were generated by assuming nucleation rates of 1 nuclei/cm^2 s and 10^{10} nuclei/cm^2 s (the value of the logarithmic term in equation (1) correspondingly ranged from 37 to 60). The theoretical variation of T with P_0 is essentially linear and is qualitatively confirmed, for the most part, by our measurements.

The predicted nucleation temperatures corresponding to $J = 1$ are in fair agreement with the data at pressures up to about 1.3 MPa. The remainder of the measurements seem to be well predicted by the calculations corresponding to a nucleation rate of 10^{10}. Such a high rate may be unrealistic for our experiment. As such, we preferred to view J as a parameter which could be freely varied and which would only weakly affect the theoretical nucleation pressure. In any case the predicted nucleation temperatures corresponding to $J = 1$ at a given pressure are within 2% of the experimental temperatures over the whole temperature range in which the experiments were performed. The nucleation pressures are less well predicted at a given temperature, particularly at temperatures approaching 570 K.

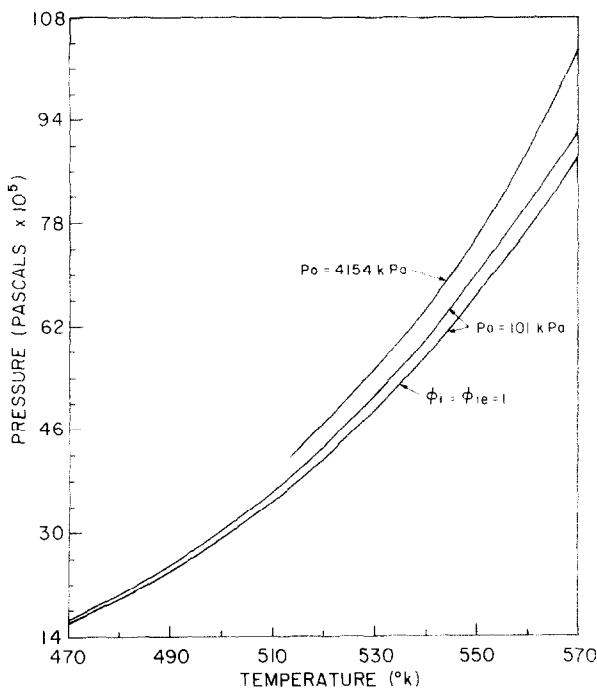There is a possibility that nucleation from unwetted

FIG. 9. Vapor pressure within a bubble at the water–n-decane interface assuming immiscibility.

solid particles attached to the water–hydrocarbon interface or nucleation of air bubbles or dissolved gases within the water drops could have produced the boiling modes shown in Figs. 2 and 3. For example, the single bubble mode illustrated in Fig. 2 is qualitatively similar to the type of boiling reported by Sideman and Taitel [30] for n-pentane drops vaporizing in distilled water. The relation of the theoretical predictions to the measurements shown in Figs. 5 and 6 is also somewhat consistent with the generally observed trend that the solubility of a gas in a liquid usually decreases with increasing temperature. However, the relatively high superheats sustained by the water drops before they boiled is some evidence of the success in minimizing the effect of such extraneous nucleation aids.

The above results may be useful for determining whether or not internal boiling (i.e., microexplosion [3]) can be initiated within water-in-fuel emulsified droplets during combustion at high ambient pressures. In the case of immiscible water and hydrocarbon, such boiling will be initiated if the droplet temperature (T_d) surpasses the temperature (T) at which critical size nuclei are most likely to form at the interface between dispersed water drops and surrounding fuel within the emulsion. On the other hand, if $T > T_d$, in which case boiling within a burning emulsified fuel droplet would not be expected, increasing P_0 will in turn increase T_d. Whether or not this increase will enhance the likelihood for nucleation of bubbles within the emulsified drop depends on how strongly T and T_d depend on ambient pressure. For example, assume for an upper limit that $T_d \simeq T_{2e}$. Then from Figs. 4–6 it is seen that

$dT_{2e}/dP_0 > dT/dP_0$. (This result is also applicable to a fuel drop which is a miscible solution of liquids [31].) The critical pressure above which $T_{2e} > T$ lies approximately between 0.3 MPa and 0.4 MPa in the water–n-decane system as illustrated in Fig. 4 (assuming immiscibility is valid). For the other two, relatively nonvolatile, hydrocarbons which were studied, it is below atmospheric pressure. Therefore, by increasing the ambient pressure of combustion, one might expect that an emulsified fuel droplet which does not undergo microexplosion at a low pressure could, however, burn disruptively at another higher pressure simply because the droplet burning temperature (i.e. the saturation temperature of the continuous phase in our present approximation) will be driven up past the nucleation temperature attendant to the increase in P_0.

It should be pointed out that by increasing the ambient pressure, the bubble growth rate and hence the intensity of the microexplosion may be reduced. The diffusion of water in fuel due to solubility effects could also be appreciable at increased temperatures and pressures. This effect would be most pronounced when the steady state droplet burning temperature is greater than the critical solution temperature of water and fuel. A water–fuel emulsion prepared at a temperature low enough that the components exhibit low mutual solubility could then become a miscible solution of water and fuel at another higher temperature. Disruptive combustion would then be initiated only when the droplet burning temperature exceeded the limit of superheat of the appropriate water–fuel solution. This latter temperature is higher than that

calculated by assuming immiscibility. (These concepts may be more relevant for fuel blends whose components have fairly low critical solution temperatures such as, for example, blends of the normal alcohols and normal paraffins.) The practical benefits which are usually attributed to this secondary atomization process may therefore, in fact, not be realized at high pressures. These concepts could be important with respect to burning emulsified fuels in diesel engines.

4. CONCLUSIONS

The boiling of water drops within nonvolatile liquid paraffins was found to occur at the water–hydrocarbon interface at both atmospheric and elevated pressures, as predicted by consideration of the surface and interfacial free energies of water and hydrocarbon. The relatively high superheats observed before nucleation of bubbles occurred were explained by a model for homogeneous nucleation which assumed that the initial bubbles whose subsequent growth leads to the observed boiling effect formed at the water–hydrocarbon interface. The nucleation temperatures were found to be relatively insensitive to pressure compared to the variation of the hydrocarbon saturation temperature with pressure, which was in qualitative agreement with the theory. And lastly, observations qualitatively revealed that the solubility of water in the hydrocarbons could strongly influence the nucleation pressure.

REFERENCES

1. W. M. Porteous and R. C. Reid, Light hydrocarbon vapor explosions, Chem. Engng Prog. 12, 83–89 (1976).
2. A. G. Newlands and W. D. Halstead, The reaction between water and molten sodium, Int. J. Heat Mass Transfer 21, 897–903 (1978).
3. J. C. Lasheras, A. C. Fernandez-Pello and F. L. Dryer, Initial observations on the free droplet combustion characteristics of water-in-fuel emulsions, Combust. Sci. Technol. 21, 1–14 (1979).
4. M. Blander and J. L. Katz, Bubble nucleation in liquids, A.I.Ch.E. Jl 21, 833–848 (1975).
5. R. E. Apfel, Vapor cavity formation in liquids, Technical Memorandum 62. Harvard University, Acoustics Research Laboratory (1970).
6. G. R. Moore, Vaporization of superheated drops in liquids, Ph.D. Thesis. University of Wisconsin (1956).
7. T. J. Jarvis, M. D. Donohue and J. L. Katz, Bubble nucleation mechanisms of liquid drops superheated in other liquids, J. Coll. Interface Sci. 50, 359–368 (1975).
8. F. C. H. Jongenelen, F. Groeneweg and J. H. Gouda, Effects of interfacial forces on the evaporation of a superheated water droplet in a hot immiscible oil, Chem. Engng Sci. 33, 777–781 (1978).
9. M. Blander, D. Hengstenberg and J. L. Katz, Bubble nucleation in n-pentane, n-hexane, n-pentane + n-hexadecane mixtures, and water, J. Phys. Chem., Ithaca 75, 3613–3619 (1971).
10. J. G. Eberhart, W. Kremsner and M. Blander, Metastability limits of superheated liquids: bubble nucleation temperatures of hydrocarbons and their mixtures, J. Coll. Interface Sci. 50, 369–378 (1975).
11. T. W. Forest and C. A. Ward, Effect of a dissolved gas on the homogeneous nucleation pressure of a liquid, J. Chem. Phys. 66, 2322–2330 (1977).
12. T. W. Forest and C. A. Ward, Homogeneous nucleation of bubbles in solutions at pressures above the vapor pressure of the pure liquid, J. Chem. Phys. 69, 2221–2230 (1978).
13. C. T. Avedisian, Superheating and boiling of water in hydrocarbons and of hydrocarbon mixtures, Ph.D. Thesis. Princeton University (1980).
14. Y. H. Mori and K. Komotori, Boiling modes of volatile liquid drops in an immiscible liquid depending on degree of superheat, ASME Paper No. 76-HT-13 (1976).
15. M. Volmer, Kinetik der Phasenbildung, translated by U.S. Department of Intelligence, refer to ATI No. 81935 (F-TS-7068-RE) from the Clearinghouse for Federal and Technical Information (1939).
16. J. Frenkel, Kinetic Theory of Liquids. Oxford University Press, London (1946).
17. E. Dickinson, The influence of chain length on the surface tensions of oligomeric mixtures, J. Coll. Interface Sci. 53, 467–475 (1975).
18. E. Schmidt, Properties of Water and Steam in S-I Units, p. 172. Springer-Verlag, New York (1969).
19. R. Aveyard and D. A. Haydon, Thermodynamic properties of aliphatic hydrocarbon/water interfaces, Trans. Faraday Soc. 61, 2255–2261 (1965).
20. H. Y. Jennings, The effect of temperature and pressure on the interfacial tension of benzene–water and normal decane–water, J. Coll. Interface Sci. 24, 323–329 (1967).
21. J. F. Connolly, Solubility of hydrocarbons in water near the critical solution temperatures, J. Chem. Engng Data 11, 13–16 (1966).
22. R. G. Sultanov, V. G. Skripka and A. Yu Namiot, Phase equilibrium in the n-hexadecane–water system at high temperatures, Russ. J. Phys. Chem. 45, 1526 (1971).
23. R. E. Apfel, Water superheated to 279.5°C at atmospheric pressure, Nat. Phys. Sci. 238, 63–64 (1972).
24. D. Y. Peng and D. B. Robinson, A new two-constant equation of state, Ind. Engng Chem. 15, 59–64 (1976).
25. D. Y. Peng and D. B. Robinson, Two and three phase equilibrium calculations for systems containing water, Can. J. Chem. Engng 54, 595–599 (1976).
26. E. W. Lykman, C. A. Eckert and J. M. Prausnitz, Generalized reference fugacities for phase equilibrium thermodynamics, Chem. Engng Sci. 20, 685–691 (1965).
27. M. Gómez-Nieto and G. Thodos, Generalized vapor pressure equation for non-polar substances, Ind. Engng Chem. Fund. 17, 45–51 (1978).
28. J. H. Keenan, F. G. Keyes, P. G. Hill and J. G. Moore, Steam Tables, p. 141. Wiley, New York (1969).
29. R. W. Hankinson and G. H. Thomson, A new correlation for saturated densities of liquids and their mixtures, A.I.Ch.E. Jl 25, 653–663 (1979).
30. S. Sideman and Y. Taitel, Direct-contact heat transfer with change of phase: evaporation of drops in an immiscible liquid medium, Int. J. Heat Mass Transfer 7, 1273–1289 (1964).
31. C. T. Avedisian and I. Glassman, High pressure homogeneous nucleation of bubbles within superheated binary liquid mixtures, J. Heat Transfer (to be published).

706   C. T. Avedisian and I. Glassman

EBULLITION ET SURCHAUFFE DE L'EAU DANS LES HYDROCARBURES AUX PRESSIONS FORTES

Résumé—L'ébullition de gouttes d'eau surchauffées dans quelques n-alkanes non volatils est étudiée expérimentalement à des pressions allant jusquà 4 MPa. On trouve que l'ébullition est initiée à l'interface eau/hydrocarbure soit par croissance d'une bulle unique soit par des chapelets de bulles qui partent de l'interface. La température d'apparition de l'ébullition est relativement indépendante de la pression, croissant seulement de 40 K pour un changement de pression de 4 MPa.

Une théorie qualitative basée sur la nucléation homogène des bulles dans les liquides surchauffés est utilisée pour expliquer l'effet de la pression sur la température d'ébullition. Les deux modes d'ébullition observés sont justifiés en considérant les énergies libres de surface et interfaciales de l'eau et de l'hydrocarbure, et on trouve un accord qualitatif entre les variations calculées et mesurées de la pression de nucléation en fonction de la température. L'information est utilisée pour éclairer le mécanisme de 'microexplosion' de gouttelettes d'eau en émulsion dans un fuel, qui apparaît à pression élevée.

ÜBERHITZUNG UND SIEDEN VON WASSER IN KOHLENWASSERSTOFFEEN BEI HOHEN DRÜCKEN

Zusammenfassung—Es wird das Sieden von überhitzten Wassertropfen untersucht. Die Tropfen befinden sich – bei Drücken bis zu 4 MPa – in flüssigen, nicht flüchtigen n-Alkanen. Es zeigte sich, daß das Sieden an der Wasser-/Kohlenwasserstoff-Grenzfläche beginnt, und zwar entweder durch das Wachsen von Einzelblasen oder durch Blasenströme, welche von der Phasengrenzfläche ausgehen. Die Temperatur, bei der das Sieden beginnt, ist nur wenig abhängig vom Druck, sie nahm bei einer Änderung des Drucks um 4 MPa nur um 40 K zu.

Der Einfluß des Siededrucks auf die Temperatur wird mit einer Theorie erklärt, welche auf der homogenen Keimbildungstheorie aufbaut. Die zwei Arten des Siedens können erklärt werden durch die freien Oberflächenenergien von Wasser und Kohlenwasserstoff. Gemessene und berechnete Ändergungen der Temperatur mit dem Druck, bei dem das Sieden einsetzt, stimmen qualitativ überein. Die erhaltenen Informationen ermöglichen es, die Vorgänge genauer zu verstehen, die bei der disruptiven Verbrennung oder der Mikroexplosion von Wasser-Heizöl-Emulsionen bei der Verbrennung unter hohem Druck auftreten.

ПЕРЕГРЕВ И КИПЕНИЕ ВОДЫ В УГЛЕВОДОРОДАХ ПРИ ВЫСОКОМ ДАВЛЕНИИ

Аннотация — Экспериментально исследовалось кипение перегретых водяных капель в некоторых нелетучих жидких н-алканах при давлении окружающей среды до 4 МПа. Показано, что кипение возникает на границе раздела вода-углеводород и проявляется в виде роста единичного пузырька или в появлении цепочек пузырьков, поднимающихся с поверхности раздела. Найдено, что температура, при которой возникает кипение, почти не зависит от давления, так как увеличивается только примерно на 40 К при изменении давления на 4 МПа. Для объяснения влияния давления на температуру кипения используется качественная теория однородного зарождения пузырьков внутри перегретых жидкостей. Оба режима кипения описываются исходя из свободных энергий воды и углеводородов на поверхности и на границе раздела. Измеренные значения качественно согласуются с результатами расчетов влияния температуры на величину давления, при котором происходит образование центров кипения. Полученные данные использовались для выяснения механизма прерывистого горения или «микровзрывов» горящих капель топливно-водной эмульсии в случае ее сжигания при высоком давлении.